

基于支持向量回归机的汽轮机排汽焓预测研究

米 兰¹,王文斌²

(1. 乌海职业技术学院,内蒙古 乌海 016000; 2. 雅砻江流域水电开发有限公司 四川 成都 610051)

摘 要:针对现有汽轮机排汽焓计算方法尤其是神经网络预测方法存在的网络结构不好确定、易陷入局部极值等不足,本文提出了一种新的基于支持向量回归机的汽轮机排汽焓预测方法。在分析了汽轮机排汽焓预测主要影响因素的基础上,为了简化计算流程提高预测的有效性,输入参数中排除了也可能处于湿蒸汽区的7、8段抽汽焓,进一步构建了基于支持向量回归机的汽轮机排汽焓预测模型。应用实例的仿真结果表明,该方法具有较强的泛化能力,可以快速、准确地完成汽轮机排汽焓在线预测。

关键词:汽轮机;排汽焓;支持向量机;支持向量回归机
中图分类号:TK262 文献标识码:A
DOI:10.16146/j.cnki.rndlgc.2016.11.007

引 言

在监测热电厂汽轮机运行状态、衡量汽轮机性能、评估热力系统热经济性等方面,都需要科学对汽轮机的排汽焓进行计算。由于汽轮机的排汽点处于湿蒸汽区,在线测量蒸汽湿度的手段尚不具备,又不能仅通过温度和压力两个因素来计算排汽焓,因此,如何准确实时计算汽轮机的排汽焓成为了汽轮机理论研究和工程实践中的难点问题。目前,计算汽轮机的排汽焓主要有曲线外推法、能量平衡法、余速损失法、焓增算法和电算迭代法等方法,但这些方法均存在不同程度上的局限性。因此,许多学者尝试采用不同形式的神经网络方法来预测汽轮机的排汽焓,并取得了较好的效果^[1~6]。但是,神经网络方法存在一些不可避免的缺陷,如网络结构难以确定、局部极值、收敛速度慢、过学习、推广能力较差和需要大量数据样本进行训练等问题。此外,现有基于神经网络的汽轮机排汽焓预测方法均将也可能处于湿蒸汽区的7、8段抽汽焓作为神经网络的第一层或第二层输入,一定程度上增加了计算量并降低了有效性。

支持向量机(Support Vector Machine, SVM)是V. Vapnik等人于20世纪90年代在统计学习理论的基础上发展起来的一种新型机器学习算法,克服了神经网络方法很多固有的缺陷。它通过结构风险最小化准则取得实际风险,较好地解决了以往许多学习方法中小样本、非线性和高维数等难题,在预测、模式识别、系统辨识、故障诊断、优化控制和数据挖掘等领域得到了广泛的应用^[7~9]。支持向量回归机(Support Vector Regression, SVR)是支持向量机在回归领域的应用,它被广泛应用于各种预测问题并取得了理想的效果。鉴于此,本研究尝试采用支持向量回归机来解决热电厂汽轮机排汽焓的预测问题。

1 影响汽轮机排汽焓预测的主要因素

由于热电厂汽轮机的工作环境复杂恶劣,所以影响汽轮机排汽焓的因素较多,相互之间的关系也较为复杂。通过分析可知,汽轮机排气焓与各主要影响因素之间的关系可表示为^[4]:

$$h = f(D, p_e, p_c, h_i, \theta_i, t_r) \quad (1)$$

式中: D —机组的主蒸汽流量, $\mu\text{t/h}$; p_e —机组的发电量, kW ; p_c —汽轮机的排气压力, kPa ; h_i —汽轮机的进气及各段抽汽焓值, kJ/kg ; θ_i —机组各加热器端差, $^{\circ}\text{C}$; t_r —再热蒸汽的温度, $^{\circ}\text{C}$ 。

在汽轮机排汽焓预测问题中,通常采用主蒸汽流量、发电量、主蒸汽焓值、1~8段抽汽焓值作为输入参数,由于7、8段抽气也可能处于湿蒸汽区,若采用7、8段抽气焓值,则可能会产生较大的不确定性和计算误差。为了提高预测的有效性和可靠性,本文选用主蒸汽流量、发电量、主蒸汽焓值、1~6段抽汽焓值作为影响汽轮机排汽焓预测的主要因素。

收稿日期:2015-08-21; 修订日期:2015-11-16

基金项目:“十二五”国家科技支撑计划项目(2014BAD06B00)

作者简介:米 兰(1981-),女,内蒙古赤峰人,乌海职业技术学院讲师。

2 支持向量回归机算法

支持向量机最初是用来做分类的,为了能够解决回归估计问题,需要借助 ε 不敏感损失函数来实现^[10~11]。首先考虑用线性回归函数 $f(x) = (w \cdot x) + b$ 估计训练样本集 $D = \{(x_i, y_i)\}, i = 1, 2, \dots, n$, $x_i \in R^d, y_i \in R$ 。假设所有训练数据在精度 ε 下无误差地用线性函数拟合,即:

$$\begin{cases} y_i - w \cdot x_i - b \leq \varepsilon \\ w \cdot x_i + b - y_i \leq \varepsilon \end{cases} \quad i = 1, 2, \dots, n \quad (2)$$

则优化目标为:

$$\min \frac{1}{2} \|w\|^2 \quad (3)$$

考虑到允许拟合误差情况,引入松弛变量 $\xi_i \geq 0$ 和 $\xi_i^* \geq 0$, 则式(3)变为:

$$\begin{cases} y_i - w \cdot x_i - b \leq \varepsilon + \xi_i \\ w \cdot x_i + b - y_i \leq \varepsilon + \xi_i^* \end{cases} \quad i = 1, 2, \dots, n \quad (4)$$

式(4)的优化目标变为:

$$\min \left\{ \frac{1}{2} \|w\|^2 + C \sum_{i=1}^n (\xi_i + \xi_i^*) \right\} \quad (5)$$

式中:右边的第一项是为了提高学习的泛化能力;第二项则为减少误差,常数 $C > 0$ 对两者做出折衷,表示对超出误差 ε 的样本的惩罚程度。根据 ε 不敏感损失函数定义知,当 $f(x_i) = (w \cdot x_i) + b$ 与 y_i 的差别不大于 ε 时,不计误差,即为零,当大于 ε 时,误差为 $|f(x_i) - y_i| - \varepsilon$,也可以看出此时得到的最优化问题也具有稀疏特性。以上的数学问题是一个凸二次规划问题,为了求解,构造 Lagrange 函数:

$$\begin{aligned} L(w, \xi_i^*, \xi_i) = & \frac{1}{2} \|w\|^2 + C \sum_{i=1}^n (\xi_i^* + \xi_i) - \\ & \sum_{i=1}^n \alpha_i^* [\xi_i^* + \varepsilon + y_i - w \cdot x_i - b] - \sum_{i=1}^n \alpha_i [\xi_i + \varepsilon - y_i \\ & + (w \cdot x_i + b)] - \sum_{i=1}^n (\gamma_i^* \xi_i^* + \gamma_i \xi_i) \end{aligned} \quad (6)$$

式中: $\alpha_i, \alpha_i^* \geq 0, \gamma_i, \gamma_i^* \geq 0, i = 1, 2, \dots, n$ 。

求解上式即对 w, b, ξ_i^* 和 ξ_i 求导数,有:

$$\begin{cases} \frac{\partial L}{\partial w} = 0 \rightarrow w = \sum_{i=1}^n (\alpha_i^* - \alpha_i) x_i \\ \frac{\partial L}{\partial b} = 0 \rightarrow \sum_{i=1}^n (\alpha_i - \alpha_i^*) = 0 \\ \frac{\partial L}{\partial \xi_i^*} = 0 \rightarrow C - \alpha_i^* - \gamma_i^* = 0 \\ \frac{\partial L}{\partial \xi_i} = 0 \rightarrow C - \alpha_i - \gamma_i = 0 \end{cases} \quad (7)$$

将上式代入式(6),有:

$$\begin{aligned} L(w, \xi_i^*, \xi_i) = & -\varepsilon \sum_{i=1}^n (\alpha_i^* + \alpha_i) + \sum_{i=1}^n y_i (\alpha_i^* - \\ & \alpha_i) - \frac{1}{2} \sum_{i=1}^n \sum_{j=1}^n (\alpha_i^* - \alpha_i) (\alpha_j^* - \alpha_j) (x_i \cdot x_j) \end{aligned} \quad (8)$$

因此,根据 Wolf 对偶的定义,在 KKT 条件下,得到 Lagrange 的对偶形式为:

$$\begin{aligned} \max W(\alpha^*, \alpha) = & -\varepsilon \sum_{i=1}^n (\alpha_i^* + \alpha_i) + \sum_{i=1}^n y_i (\alpha_i^* \\ & - \alpha_i) - \frac{1}{2} \sum_{i=1}^n \sum_{j=1}^n (\alpha_i^* - \alpha_i) (\alpha_j^* - \alpha_j) (x_i \cdot x_j) \end{aligned} \quad (9)$$

$$s. t. \quad \sum_{i=1}^n (\alpha_i - \alpha_i^*) = 0, 0 \leq \alpha_i, \alpha_i^* \leq C, i = 1, 2, \dots, n$$

得到的回归函数为:

$$f(x) = (w \cdot x) + b = \sum_{i=1}^n (\alpha_i^* - \alpha_i) (x_i \cdot x) + b \quad (10)$$

对于非线性问题,可通过非线性变换转化为某个高维空间中的线性问题,即用核函数 $K(x_i, x_j)$ 替代原来的内积运算 $(x_i \cdot x_j)$,就可以实现非线性函数拟合:

$$f(x) = w^T \varphi(x) + b = \sum_{i=1}^n (\alpha_i^* - \alpha_i) K(x_i \cdot x) + b \quad (11)$$

核函数 $K(x, y)$ 的形式有多种,比如^[11]:

(1) 多项式核函数: $K(x, y) = (x \cdot y + 1)^d$;

(2) sigmoid 感知核函数: $K(x, y) = \tanh[k(x \cdot y) + \theta]$;

(3) 径向基核函数: $K(x, y) = \exp\left(-\frac{\|x - y\|^2}{2\sigma^2}\right)$;

(4) 多二次曲面核函数: $K(x, y) = \frac{1}{\sqrt{\|x - y\|^2 + c^2}}$;

3 基于支持向量回归机的汽轮机排汽焓预测模型

在分析汽轮机排汽焓预测主要影响因素和介绍支持向量回归机算法的基础上,构建基于支持向量回归机的汽轮机排汽焓预测模型,具体步骤为:

(1) 分析汽轮机排汽焓的影响因素,确定支持

向量回归机的输入输出参数。通过前面的分析可知,确定主蒸汽流量、发电量、主蒸汽焓值、1~6段抽汽焓值为输入参数,汽轮机排汽焓为输出参数。

(2) 对训练样本和要预测的样本数据进行规范化处理。这里采用公式 $\bar{x}_{ij} = x_{ij}/x_{i\max}$ 对数据进行规范化处理,其中 x_{ij} 表示第 i 个输入参数在第 j 种工况下的数值, $x_{i\max}$ 表示第 i 个输入参数所有工况下的最大值。

(3) 选择合适的支持向量回归机核函数。通过对比分析,选用预测效果较为理想的径向基核函数。

(4) 利用支持向量回归机对训练样本进行训练,不断调整不敏感值 ε 、正则化参数 C 和径向基核函数的宽度参数 σ ,直到训练误差达到满足精度

要求为止。

(5) 利用支持向量回归机对一定工况下的汽轮机排汽焓进行预测。

4 应用实例

为了验证所建立模型的有效性,以文献[5]中的仿真数据为依据。已知某热电厂300 MW机组最大负荷、额定负荷、85%负荷、70%负荷、60%负荷、50%负荷和40%负荷工况下的主要原始数据如表1所示,其中的数据为运行和实验所得^[5]。按照预测模型中 Step 2 的数据规范化方法,可以得到如表2所示的规范化输入输出参数。

表1 主要原始数据

Tab.1 Main original data

参 数	最大负荷	额定负荷	85% 负荷	70% 负荷	60% 负荷	50% 负荷	40% 负荷
主蒸汽流量/t·h ⁻¹	1 025.0	935.0	768.0	624.5	446.2	393.6	341.2
发电量/MW	326	300	255	210	180	150	120
主蒸汽焓/kJ·kg ⁻¹	3 387.8	3 397.3	3 400.3	3 433.7	3 453.4	3 473.0	3 444.2
1 段抽汽焓/kJ·kg ⁻¹	3 150.5	3 152.8	3 130.5	3 159.1	3 175.1	3 191.0	3 195.2
2 段抽汽焓/kJ·kg ⁻¹	3 027.8	3 030.9	3 013.6	3 039.7	3 052.3	3 068.9	3 076.4
3 段抽汽焓/kJ·kg ⁻¹	3 329.4	3 332.3	3 338.0	3 339.0	3 333.3	3 331.6	3 330.6
4 段抽汽焓/kJ·kg ⁻¹	3 128.0	3 131.0	3 136.6	3 138.8	3 135.6	3 132.4	3 130.7
5 段抽汽焓/kJ·kg ⁻¹	2 933.6	2 936.3	2 941.5	2 943.8	2 941.6	2 939.3	2 938.5
6 段抽汽焓/kJ·kg ⁻¹	2 753.5	2 755.8	2 760.1	2 762.6	2 760.4	2 759.3	2 760.8
排汽焓/kJ·kg ⁻¹	2 345.8	2 375.7	2 373.5	2 392.4	2 406.9	2 421.3	2 427.5

表2 规范化输入输出参数

Tab.2 Standardized input and output parameters

参 数	最大负荷	额定负荷	85% 负荷	70% 负荷	60% 负荷	50% 负荷	40% 负荷
主蒸汽流量/t·h ⁻¹	1.0000	0.9122	0.7493	0.6093	0.4353	0.3840	0.3329
发电量/MW	1.0000	0.9202	0.7822	0.6442	0.5521	0.460	0.3681
主蒸汽焓/kJ·kg ⁻¹	0.9755	0.9782	0.9791	0.9887	0.9944	1.0000	0.9917
1 段抽汽焓/kJ·kg ⁻¹	0.9860	0.9867	0.9798	0.9887	0.9937	0.9987	1.0000
2 段抽汽焓/kJ·kg ⁻¹	0.9842	0.9852	0.9796	0.9881	0.9922	0.9976	1.0000
3 段抽汽焓/kJ·kg ⁻¹	0.9971	0.9980	0.9997	1.0000	0.9983	0.9978	0.9975
4 段抽汽焓/kJ·kg ⁻¹	0.9966	0.9975	0.9993	1.0000	0.9990	0.9980	0.9974
5 段抽汽焓/kJ·kg ⁻¹	0.9965	0.9975	0.9992	1.0000	0.9993	0.9985	0.9982
6 段抽汽焓/kJ·kg ⁻¹	0.9967	0.9975	0.9991	1.0000	0.9992	0.9988	0.9993
排汽焓/kJ·kg ⁻¹	0.9663	0.9787	0.9778	0.9855	0.9915	0.9974	1.0000

这里将最大负荷、额定负荷、85% 负荷、70% 负荷、60% 负荷和 40% 负荷工况下的数据作为训练样本。采用 MATLAB 软件并调用支持向量机工具箱,编写基于支持向量回归机的汽轮机排汽焓预测模型。通过对规范化训练样本的训练,最终将支持向量回归机的相关参数分别设置为: $\varepsilon = 0.0001$, $C = 1000$, $\sigma = 10$ 。经过计算,可以得出如表 3 所示的 6 种工况下训练样本排汽焓的预测误差,从中不难看出,所建立的支持向量回归机预测模型的训练效果非常好,准确性较高。

表 3 训练样本的预测误差

Tab.3 Errors of the training specimen predicted

负 荷	计算值/ kJ · kg ⁻¹	预测值/ kJ · kg ⁻¹	绝对误差/ kJ · kg ⁻¹	相对误 差/%
最大负荷	2 345.8	2 345.9	0.1	0.004
额定负荷	2 375.7	2 375.3	0.4	0.017
85% 负荷	2 373.5	2 373.8	0.3	0.013
70% 负荷	2 392.4	2 392.5	0.1	0.004
60% 负荷	2 406.9	2 406.6	0.3	0.012
40% 负荷	2 427.5	2 427.3	0.2	0.008

为了检验所建立的预测模型的泛化能力,将 50% 负荷工况下的数据作为校验样本进行预测,预测结果与文献 [5] 采用双隐层 RBF 过程神经网络的预测结果列于表 4。通过表 4 可以看出,基于支持向量回归机的汽轮机排汽焓预测模型具有较强的泛化能力,预测的精度高于双隐层 RBF 过程神经网络预测模型。为了说明 7、8 段抽气焓对预测结果的影响,将预测模型的输入参数中加上 7、8 段抽气焓,可以得到 50% 负荷工况下的预测值为 2 417.6 kJ/kg,可见预测误差大于不考虑 7、8 段抽气焓时的情形。以往的神经网络预测方法将可能处于湿蒸汽区的 7、8 段抽气焓作为网络输入或是双层神经网络第一级的输出,不仅增加了不确定性还增加了网络的复杂性。支持向量回归机非常适合解决小样本、输入参数较少的预测问题,本文建立的预测模型去除了可能处于湿蒸汽区的 7、8 段抽气焓,在保证预测精度的前提下不仅降低了测试过程带来的不确定性,同时也简化了计算过程。

表 4 50% 负荷工况时两种方法对排汽焓的预测结果比较

Tab.4 Comparison of the results of the exhaust steam enthalpy predicted by using both methods under the operating condition at the 50% load

预测方法	计算值/kJ · kg ⁻¹	预测值/kJ · kg ⁻¹	绝对误差/kJ · kg ⁻¹	相对误差/%
双隐层 RBF 过程神经网络	2 421.3	2 420.41	0.89	0.037
支持向量回归机	2 421.3	2 421.96	0.66	0.027

5 结 论

本文提出了一种基于支持向量回归机的汽轮机排汽焓预测方法,该方法具有适应性强、全局优化、训练时间短、泛化性能好和抗干扰能力强等特点,在预测模型的输入参数方面,取消了以往预测方法中可能降低预测效果的 7、8 段抽气焓。应用实例的预测结果表明,所建立的基于支持向量回归机的汽轮机排汽焓预测模型具有较强的泛化能力和较高的预测精度,预测结果完全满足在线监测和分析的工程实际需要,具有较大的工程实用价值和理论意义。

参考文献:

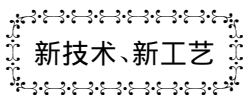
[1] 郭江龙,张树芳,陈海平.基于 BP 神经网络的汽轮机排汽焓在线计算方法[J].热能动力工程,2004,19(2):179-183.
GUO Jiang-long, ZHANG Shu-fang, CHEN Hai-ping. On-line method for calculating the exhaust steam enthalpy of a steam turbine based on a BP neural network[J]. Journal of Engineering for Thermal Energy and Power 2004, 19(2):179-183.

[2] 高俊如,丁光彬,孟鑫等.利用层次径向基神经网络的汽轮机排汽焓计算[J].动力工程,2005,25(4):466-469.
GAO Jun-ru, DING Guang-bin, MENG Xin, et al. Calculation of the exhaust steam enthalpy of a steam turbine by making use of a hierarchical radial basis neural network [J]. Power Engineering, 2005, 25(4):466-469.

[3] 孟鑫,丁光彬,唐蕾.基于双并人工神经网络的汽轮机

- 排汽焓计算[J]. 汽轮机技术, 2006, 48(1):14-16.
MENG Xin, DING Guang-bin, TANG Lei. Calculation of the exhaust steam enthalpy of a steam turbine based on dual parallel artificial neural network [J]. Steam Turbine Technology, 2006, 48(1):14-16.
- [4] 张利平, 王铁生. 基于免疫原理的 RBF 神经网络模型在汽轮机排汽焓计算中的应用[J]. 汽轮机技术, 2008, 50(5):347-349.
ZHANG Li-ping, WANG Tie-sheng. Applications of a RBF neural network model based on the immune theory in calculation of the exhaust steam enthalpy of a steam turbine [J]. Steam Turbine Technology, 2008, 50(5):347-349.
- [5] 官唤春. 基于双隐层径向基过程神经网络的汽轮机排汽焓在线预测[J]. 热力发电, 2014, 43(7):32-35.
GONG Huan-chun. Double hidden layer RBF process neural network based online prediction of steam turbine exhaust enthalpy [J]. Thermal Power Generation, 2014, 43(7):32-35.
- [6] 吴俊杰, 侯宏娟, 杨勇平. 神经网络算法在汽轮机排汽焓估算中的应用[J]. 热力发电, 2014, 43(8):125-129.
WU Jun-jie, HOU Hong-juan, YANU Yong-ping. Applications of the neural network-based algorithm in estimation of the exhaust steam enthalpy of a steam turbine [J]. Thermal Power Generation, 2014, 43(8):125-129.
- [7] 周璇, 杨建成. 基于支持向量回归机的空调逐时负荷滚动预测算法[J]. 中南大学学报(自然科学版), 2014, 45(3):952-955.
ZHOU Xuan, YANG Jian-cheng. An algorithm for predicting the hourly rolled load of an air conditioner based on the SVR machine [J]. Journal of Central South University (Natural Science Edition), 2014, 45(3):952-955.
- [8] 傅贵, 韩国强, 逯峰, 等. 基于支持向量机回归的短时交通流预测模型[J]. 华南理工大学学报(自然科学版), 2013, 41(9):71-76.
FU Gui, HAN Guo-qiang, LU Feng, et al. Short-time traffic flow forecasting model based on the regression in a support vector machine [J]. Journal of South China University of Technology (Natural Science Edition), 2013, 41(9):71-76.
- [9] 周文明, 陈军生, 宋吉星, 等. 基于支持向量机的装备技术准备能力预测算法[J]. 系统工程与电子技术, 2013, 35(9):1903-1907.
ZHOU Wen-ming, CHEN Jun-sheng, SONG Ji-xing, et al. Algorithm for predicting the technical preparation capacity of armament based on a supporting vector machine [J]. Systematic Engineering and Electronic Technology, 2013, 35(9):1903-1907.
- [10] 方瑞明. 支持向量机理论及其应用分析[M]. 北京: 中国电力出版社, 2007.
FANG Rui-ming. Supporting vector machine theory and analysis of its applications [M]. Beijing: China Electric Power Press, 2007.
- [11] 李应红, 尉询楷, 刘建勋. 支持向量机的工程应用[M]. 北京: 兵器工业出版社, 2004.
LI Ying-hong, WEI Xun-kai, LIU Jian-xun. Engineering application of supporting vector machines [M]. Beijing: Weapon Industry Press, 2004.

(刘瑶 编辑)



坦普尔 755 MW 联合循环装置商业交工试运转

据《Gas Turbine World》2014 年 9~10 月刊报道, 得克萨斯 Randa Power 独立电力生产商的“Flex Plant”装置是按快速启动和升/降负荷而设计的。

这也是 Siemens“成形电力”在美国的首次应用, 在高环境温度下运行时, 输出功率增加 10%。

提供了该装置的工程和设计细节内容以及运行。

(吉桂明 摘译)

燃气透平叶片 3 种出气边冷却结构中流动与传热性能的比较 = **Comparison of the Flow and Heat Transfer Performance of Three Types of Trailing Edge Cooling Structure in Blades of a Gas Turbine** [刊, 汉]/LIU Zheng, CHEN Liu, DAI Ren (College of Energy Source and Power Engineering, Shanghai University of Science and Technology, Shanghai, China, Post Code: 200093) // Journal of Engineering for Thermal Energy & Power. - 2016, 31(11). - 32 ~ 37

Through a flow and heat coupling calculation and test verification, compared were the flow and heat transfer performance of the trailing edge cooling structure with cylindrical holes in a row and two types of cutback at various Reynolds numbers and cooling air mass flow rates. It has been found that the cylindrical holes in a row have an excessively high flow resistance and due to the limitation of the air supply pressure, the cooling air flow rate is excessively low and the cooling effectiveness is not good enough, leading to erosion at the trailing edge at a very high temperature. To provide a blade with a cutback film cooling structure at the trailing edge on the pressure surface can lower the flow resistance and enhance the cooling air flow rate. To adopt the chord-wise rib and pinfin cooling structure inside the slot can intensify the heat exchange and improve the cooling efficiency. At a same cooling air flow rate, the pressure difference required by the flow in the cutback cooling structure will notably drop and the width of the wake of blades in a cascade will also become small, thus favorable for reducing the flow losses and surface heat transfer in cascades at the downstream. **Key words:** cylindrical holes in a row, cutback, cooling efficiency, wake trace configuration

基于支持向量回归机的汽轮机排汽焓预测研究 = **Study of the Prediction of the Exhaust Steam Enthalpy of a Steam Turbine Based on the Supporting Vector Regression Machine** [刊, 汉]/MI Lan (Wuhai Vocational Technical College, Wuhai, China, Post Code: 016000), WANG Wen-bin (Yalong River Basin Hydropower Development Co. Ltd., Chengdu, China, Post Code: 610051) // Journal of Engineering for Thermal Energy & Power. - 2016, 31(11). - 38 ~ 42

In the light of such demerits existing in the prevailing steam turbine exhaust steam enthalpy calculation method, especially the neural network prediction method, as difficult to determine the network structure and easy to meet with a local extremum etc., proposed was a new steam turbine exhaust steam enthalpy prediction method based on the supporting vector regression machine. On the basis of analyzing the main factors influencing the prediction of the exhaust steam enthalpy of a steam turbine, to simplify the calculation flow path and enhance the prediction efficiency, the extraction steam enthalpy in the section No. 7 and 8 was excluded in the input parameters, which possibly located in the wet steam zone. On this basis, a model for predicting the exhaust steam enthalpy of a steam turbine was established based on the supporting vector regression machine. The simulation results in the cases show that the method in question has a relatively strong generalization ability and can quickly and accurately fulfill an on-line prediction of the exhaust steam enthalpy of a steam turbine. **Key words:** steam turbine, exhaust steam enthalpy, sup-

porting vector machine , supporting vector regression machine

撞击预燃室煤粉燃烧器气固两相流特性研究 = **Gas-Solid Two-Phase Flow Characteristics of the Pulverized Coal Burner with Impinging Pre-combustion Chamber** [刊 汉]/WANG Shuai ,FAN Bao-guo ,LIU Hai-yu ,JIN Yan (College of Electrical and Power Engineering ,Taiyuan University of Technology ,Shanxi Taiyuan 030024) // Journal of Engineering for Thermal Energy & Power. -2016 ,31(11). -43 ~49

The gas-solid two-phase flow characteristics of the pulverized coal burner with impinging pre-combustion chamber were numerically (by Fluent) and experimentally studied. The flow field ,fuel concentration and particle trajectories of the burner were examined under different secondary air angles. It is concluded that there is open air in the burner when the secondary air angle is (30° ~45°). The tangential and axial angles of the secondary air have an important influence on the air flow spreading angle ,vortex intensity and flow jet length. The flow field and particle trajectories become more reasonable when the secondary air angle is (5° ~20°). **Key words**: pulverized coal burner; gas-solid two-phase flow; experimental research; numerical simulation

不同金属材料与海水温度对海水结垢影响的实验研究 = **Experimental Study of the Influence of Various Metal Materials and Seawater Temperature on Seawater-caused Fouling** [刊 汉]/YANG Da-zhang ,LV Jing , QIU Yu-xin (Shanghai University of Science and Technology , Shanghai , China , Post Code: 200093) , LIU Jian-hua (Shanghai City Key Laboratory on Multi-phase Flow and Heat Transfer in Power Engineering , Shanghai , China , Post Code: 200093) // Journal of Engineering for Thermal Energy & Power. -2016 ,31(11). -50 ~54

Experimentally studied were the fouling phenomena existing in the heat exchange process of seawater and compared were the fouling characteristics of four kinds of metal in seawater , i. e. a galvanized iron plate , brass , copper and stainless steel material and changes of the amount of fouls on the surface of four kinds of metal. The test results show that the fouling morphology and amount of fouls formed in seawater are varied in metals , the galvanized iron plate has the largest amount of fouls and the copper materials have the comparatively serious corrosion but the smallest amount of fouls on the surface. A XRD (X-Ray Diffraction) and EDX (Energy Dispersive X-Ray) phase analysis was performed of the seawater-caused fouls. It has been found that the phase composition of the seawater-caused fouls formed on the surface of various metal materials is varied and the constituents of the seawater-caused fouls on the surface of a galvanized iron plate are mainly the products produced in the process of erosion and corrosion of zinc , however , those on the surface of stainless steel materials are mainly magnesia hydroxide. Changes of the amount of fouls formed on the surface of a galvanized iron plate and a brass material in seawater at 80 °C and 60 °C were compared. It has been found that the amount of fouls formed on the surface of the galvanized iron plate will increase with a decrease of the seawater temperature , however , that formed on the surface of brass materials